Journal of Russian Laser Research, Volume 32, Number 2, March, 2011

LOSS OF ATOM INTERFERENCE DUE TO A RANDOM PHASE

A. El Allati,[1,2]* M. El Baz,[1] Y. Hassouni,[1] A. Kassou Ou Ali,[1] and F. Saif[3]

[1] *Faculté des Sciences, Département de Physique*
LPT URAC 13, Université Mohammed V-Agdal
Av. Ibn Battouta, B.P. 1014, Rabat, Morocco

[2] *Center for Applied Mathematics and Physics*
National University of Science and Technology
H-12, Islamabad, Pakistan

[3] *Department of Electronics*
Quaid-i-Azam University
45320 Islamabad, Pakistan

*Corresponding author e-mail: abdou.allati@gmail.com
e-mails: elbaz@fsr.ac.ma, yassine.hassouni@gmail.com

Abstract

We suggest a model where the influence of an environment on the atom interference is associated with a random phase. The model consists of sending a two-level state atom through two cavities, both containing a standing wave field in the Bragg regime and Raman–Nath regime, respectively. In view of this model, we can visualize the loss of interference fringes if the randomness of the phase increases, and the restoration of the pattern when it decreases, as which-path information. Then, the controllable random noise acts as a decoherence that would destroy the quantum features.

Keywords: atom interference, atomic momentum state, quantum eraser, Bragg regime, Raman–Nath regime.

1. Introduction

In contrast to classical physics, the atom interference is a quantum phenomenon based on the superposition of states. Einstein and Bohr discussed this phenomenon in order to formulate the complementarity principle [1]. Later, Feynman described this phenomenon as containing the basic mystery of quantum mechanics [2]; it is impossible to obtain both interference and complete which-path information in a single experiment, and any attempt to identify the path taken by the particle serves to destroy the interference pattern. Now, it has become the subject of hectic research to explore both theoretical and experimental aspects of quantum physics. Theoretically, it is seen as a tool to understand quantum theory, illustrating the quantum superposition principle [1, 2]. Experimentally, any distinguishability between the paths of an interferometer destroys the structure of the interference fringes. In 1982, Scully and Drühl showed that the loss of interference does not depend on the uncertainty principle but depends on the quantum entanglement between the interfering particles and the measuring apparatus [3], known as the quantum

Manuscript submitted by the authors in English first on December 6, 2010 and in final form on March 21, 2011.
1071-2836/11/3202-0177

eraser. The quantum-eraser behavior has been reported in several experiments [4–12] using different versions (for details, see the review [13]).

In this paper, we propose a model that serves as a quantum eraser that can destroy and restore the atom interference. It consists of sending a two-level atom through two cavities in two different regimes (both containing a standing wave field in the Bragg regime and Raman–Nath regime, respectively). The model allows us to obtain the atom interference by the atomic external degrees of freedom and to study the effect of environment [14, 15]. The first regime is the deflection of atoms in the ground state with a field mode in the Fock state inside the first cavity, in the Bragg regime. Controlling the atom–field interaction time allows one to generate the atomic momentum states. After that, the previous atom is excited by the Ramsey field and passes through the second cavity kept in the Raman–Nath regime. The interference phenomenon is obtained through the superposition of momentum states of the atom [16–18]. However, the decoherence is usually present, which adds noisy or out-of-random phases in the way of atoms between two regimes. Then, it yields the loss of information on the momentum state, which serves to destroy the atom interference, as which-path information [4].

The paper is organized as follows.

In Sec. 2, we describe the model and present the fundamental expressions of analytical calculations. In Sec. 3, we study the impact of the random phase, which is introduced by the environment on the interference phenomenon. Finally, in Sec. 4, conclusions on the main results are given.

2. Model

Let us consider a beam of atoms in the ground state moving with the center-of-mass momentum P_{ℓ_0} towards a cavity. The inner field in the cavity is an optical standing wave of wavelength λ. One atom is injected into the cavity, the cavity is aligned along the x axis (Fig. 1), and the atom interacts with the cavity field, which is in the Fock state $|n\rangle$. Assuming large detuning between the cavity field frequency ν and the atomic transition frequency ω_0, the atom remains in the initial state without the spontaneous emission of photons. The result of the atom–field interaction is that the atom may be undeflected or deflected in the direction of the wave propagation by an even multiple of the photon momentum $\hbar k$ [19].

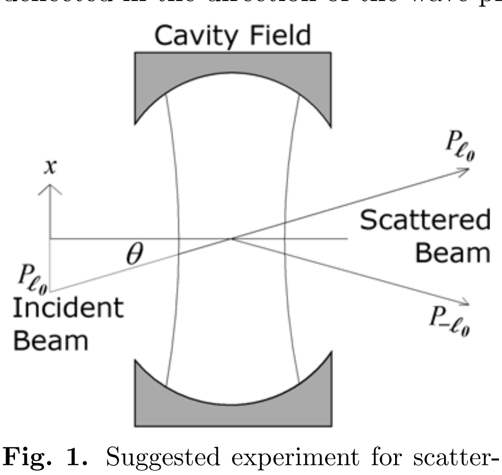

Fig. 1. Suggested experiment for scattering atoms, which is illustrated by an incoming atomic beam with momentum P_{ℓ_0} along the field and at an angle θ with respect to the vertical axis. In the Bragg regime, there are two possible directions with momentum P_{ℓ_0} and $P_{-\ell_0}$.

The total Hamiltonian of the interacting atom in the presence of its center-of-mass motion with a standing wave having a wave number k defined as $k = 2\pi/\lambda$ in the dipole and the rotating-wave approximations is given by

$$H = \frac{\hat{P}_x^2}{2M} + \frac{1}{2}\hbar\omega_0\sigma_z + \hbar\nu a^\dagger a + \hbar g \cos(k\hat{x})(\sigma_+ a + \sigma_- a^\dagger), \quad (1)$$

where $\hat{P}_x$ and $\hat{x}$ are the momentum and position operators of the atom, the operators σ_z and $\sigma_\pm$ are the Pauli matrices, a and $a^\dagger$ are the annihilation and creation operators of the standing wave, respectively, g is the atom–field coupling constant, and $\Delta = \nu - \omega_0$ describes detuning between the atomic transition frequency and the field frequency.

We suppose that the detuning is large enough, such that direct atomic transitions do not occur, but the interactions between a single atom and the cavity field in a state $|n\rangle$ do occur off resonance [23]. So, it is very rare to find the atom in the excited state. The system may be then described by the effective Hamiltonian

$$\hat{H}_{\text{eff}} = \frac{\hat{P}_x^2}{2M} - \frac{\hbar|g|^2}{2\Delta}\hat{n}\sigma_-\sigma_+ \cos(2k\hat{x}+1), \tag{2}$$

with $\sigma_+\sigma_- + a^\dagger a\sigma_z = -a^\dagger a\sigma_-\sigma_+$.

The wave function of the atom–field system, after an interaction time t, in the discrete momentum space is given by

$$|\psi(t)\rangle = \sum_{l=-\infty}^{+\infty} (C_{P_l}^{g,n}(t)|P_l, g, n\rangle + C_{P_l}^{e,n}(t)|P_l, e, n\rangle), \tag{3}$$

where $|P_l\rangle$ is the atom state of the transverse momentum P_l, $C_{P_l}^{g,n}(t)$ and $C_{P_l}^{e,n}(t)$ are the probability amplitudes that the atom exists with momentum P_ℓ after ℓ interactions, and n is the number of photons in the cavity. During the atom–field interaction, the momentum transferred to the atom by the field is either 0 or $2\hbar k$ [19], and, for each complete Rabi cycle, the momentum of the exciting atom is given by

$$P_\ell = P_{\ell_0} + \ell\hbar k, \tag{4}$$

where ℓ is an even integer.

The time evolution of the atom in the process of its interaction with the cavity field is given by the Schrödinger equation as follows:

$$i\hbar\frac{d}{dt}|\psi(t)\rangle = \hat{H}_{\text{eff}}|\psi(t)\rangle, \tag{5}$$

which leads to the following equations of motion for the probability amplitudes $C_{P_\ell}^{g,n}$:

$$i\frac{\partial C_{P_\ell}^{g,n}(t)}{\partial t} = \omega_{\text{rec}}\ell(\ell+\ell_0)C_{P_\ell}^{n}(t) - \frac{\chi^n}{2}(C_{P_\ell+2\hbar k}^{g,n}(t) + C_{P_\ell-2\hbar k}^{g,n}(t)), \tag{6}$$

where $\omega_{\text{rec}} = \hbar k^2/2M$ is the frequency associated with the photon recoil and $\chi^n = |g|^2 n/2\Delta$ is the effective Rabi frequency.

In view of Eq. (6), one can study atomic scattering through the cavity in any regime.

2.1. Bragg Regime

In the Bragg regime of atomic deflection, for large detuning [20], the recoil frequency of the atom is much higher than the effective Rabi frequency, viz.,

$$\omega_{\text{rec}} \gg \chi^n. \tag{7}$$

The energy conservation in the Bragg regime requires that

$$P_{\text{out}}^2 = (P_{\ell_0} + \ell\hbar k)^2, \tag{8}$$

where $P_{\ell_0} = [\ell_0/2]\hbar k = P_{\ell_0}$ is the initial momentum of the atom [24], and P_{out} is the atom momentum when the atom emerges out of the cavity after ℓ interactions. In the Bragg condition, $\ell_0 = 2, 4, 6\ldots$, which corresponds to the first, second, and third order of the Bragg scattering, respectively. Equation (8) has two solutions $\ell = 0$ and $\ell = -\ell_0$, which means that there exist only two possible directions of the atomic momentum out of the cavity, namely,

$$\begin{cases} \ell = 0 & \rightarrow \quad \text{undeflected}, \\ \ell = -\ell_0 & \rightarrow \quad \text{deflected}. \end{cases}$$

Substituting $|\psi(t)\rangle$ into the Schrödinger equation yields the coupled differential equations from $\ell = 0$ to $\ell = -\ell_0$ for the Bragg regime as follows:

$$\begin{aligned} i\frac{\partial C^{g,n}_{P_{\ell_0}}(t)}{\partial t} &= -\frac{\chi^n}{2}(C^{g,n}_{P_2} + C^{g,n}_{P_{-2}}), \\ i\frac{\partial C^{g,n}_{P_{-2}}(t)}{\partial t} &= \omega_{\rm rec}(-2)(-2+\ell_0)C^{g,n}_{P_{-2}}(t) - \frac{\chi^n}{2}(C^{g,n}_{P_2}(t) + C^{g,n}_{P_{-2}}(t)), \\ \cdots & \cdots \cdots \\ \cdots & \cdots \cdots \\ \cdots & \cdots \cdots \\ i\frac{\partial C^{g,n}_{-\ell_0}(t)}{\partial t} &= -\frac{\chi^n}{2}(C^{g,n}_{P_{-\ell_0+2}}(t) + C^{g,n}_{P_{-\ell_0-2}}(t)). \end{aligned} \tag{9}$$

Adiabatic solution of the coupled differential equations allows one to obtain two coupled equations [21] (for $\ell_0 > 2$):

$$i\frac{\partial C^{g,n}_{P_{\ell_0}}(t)}{\partial t} = A_n C^{g,n}_{P_{\ell_0}}(t) - \frac{1}{2}B_n C^{g,n}_{-\ell_0}(t), \tag{10}$$

$$i\frac{\partial C^{g,n}_{P_{-\ell_0}}(t)}{\partial t} = A_n C^{g,n}_{-\ell_0}(t) - \frac{1}{2}B_n C^{g,n}_{P_{\ell_0}}(t), \tag{11}$$

where

$$A_n = -\frac{(\chi^n/2)^2}{\omega_{\rm rec}(\ell_0-2)(2)} \tag{12}$$

and

$$B_n = \frac{(\chi^n)^{\ell_0/2}}{(2\omega_{\rm rec})^{(\ell_0/2)-1}[(\ell_0-2)(\ell_0)\cdots 4\cdots 2^2]}. \tag{13}$$

From Eqs. (10) and (11), the probability of the atom to exit with momentum P_{ℓ_0} is $C_{P_{\ell_0}}(t)$, and that of exiting with momentum $P_{-\ell_0}$ is $C_{-\ell_0}(t)$. So, the probability amplitudes are given, for the initial conditions $C^{g,n}_{P_{\ell_0}}(0) = 1$ and $C_{P_{-\ell_0}}(0) = 0$, by the following equations:

$$C^{g,n}_{P_{\ell_0}}(t) = e^{-iA_n t}\left[C^{g,n}_{P_{\ell_0}}(0)\cos\left(B_n(t)/2\right) + iC^{g,n}_{-\ell_0}(0)\sin\left(B_n(t)/2\right)\right], \tag{14}$$

$$C^{g,n}_{-\ell_0}(t) = e^{-iA_n t}\left[C^{g,n}_{-\ell_0}(0)\cos\left(B_n(t)/2\right) + iC^{g,n}_{P_{\ell_0}}(0)\sin\left(B_n(t)/2\right)\right]. \tag{15}$$

The substitution of these conditions in Eqs. (14) and (15) allows one to obtain the state of the scattered atom and the cavity field

$$|\psi(t)\rangle = e^{iA_n}\left[\cos\left(B_n t/2\right)|P_{\ell_0}\rangle + i\sin\left(B_n t/2\right)|P_{-\ell_0}\rangle\right]|g,n\rangle. \tag{16}$$

The probabilities that the atom exits with momentums P_{ℓ_0} and $P_{-\ell_0}$ are given by

$$\mathcal{P}(P_{\ell_0}, t) = \cos^2(B_n t/2), \tag{17}$$

$$\mathcal{P}(P_{-\ell_0}, t) = \sin^2(B_n t/2). \tag{18}$$

If the atom–cavity interaction time $t = \pi/(2B_n)$, the above probabilities are the same, and the output state of the atom state reads

$$\left|\psi\left(\frac{\pi}{2B_n}\right)\right\rangle_{\text{atom}} = \frac{1}{\sqrt{2}}[|P_{\ell_0}\rangle + |P_{-\ell_0}\rangle] \otimes |g\rangle. \tag{19}$$

The probability of finding the atom either in the state $|P_{\ell_0}\rangle$ or in the state $|P_{-\ell_0}\rangle$ is 1/2, which corresponds to the second Bragg diffraction, deflected/undeflected. After passing through the first cavity, the atom heads toward the second cavity. So, there are two possibilities for the atomic momentum states $|P_{\ell_0}\rangle$ and $|P_{-\ell_0}\rangle$. For this purpose, we suppose that the atom interacts with the field inside the second cavity, which occurs in the Raman–Nath regime.

2.2. Raman–Nath Regime

After exiting the cavity in the state (19), the atom is excited by the Ramsey field and then travels freely towards the second cavity (Fig. 2) in the state

$$|\psi\rangle_{\text{atom}} = \frac{1}{\sqrt{2}}(|P_{\ell_0}\rangle + |P_{-\ell_0}\rangle) \otimes |e\rangle, \tag{20}$$

The atom–field interaction inside the second cavity is assumed to occur at an exact resonance ($\Delta = 0$)

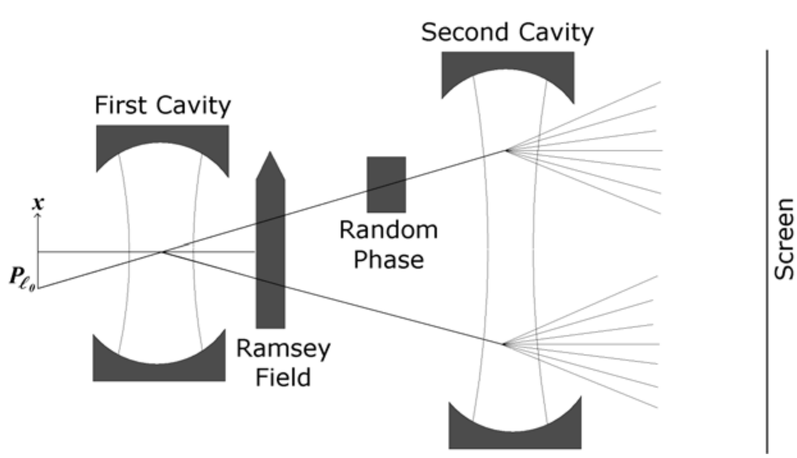

Fig. 2. Atom interference scheme with an atom passing through two cavities. Different devices such as the Ramsey field, random phase, and screen.

and is described by the Hamiltonian

$$H = \frac{\hat{P}_x^2}{2M} + \frac{1}{2}\hbar\omega_0\sigma_z + \hbar\nu a^\dagger a + \hbar g\cos(k\hat{x})(\sigma_+ a + \sigma_- a^\dagger), \tag{21}$$

where a and $a^\dagger$ are the annihilation and creation operators of the cavity mode. The effective Hamiltonian for the atom–field system is given by

$$\hat{H}_{\text{eff}} = \frac{\hat{P}_x^2}{2M} + \hbar g \cos(k\hat{x})(\sigma_+ a + \sigma_- a^\dagger). \tag{22}$$

The final state of the system after an interaction time t inside the second cavity is

$$\begin{aligned} |\psi(t)\rangle_{\text{final}} \;=\; & \frac{1}{\sqrt{2}} \sum_{\ell=-\infty}^{\infty} \left(\exp\left\{ -i \frac{P_{\ell_0}^2}{2M\hbar} t \right\} \left(C_\ell^{e,n}(t)|P_\ell, e, n\rangle + C_\ell^{g,n+1}(t)|P_\ell, g, n+1\rangle \right) \right. \\ & \left. + \exp\left\{ -i \frac{P_{-\ell_0}^2}{2M\hbar} t \right\} \left(C_{-\ell}^{e,n}(t)|P_{-\ell}, e, n\rangle + C_{-\ell}^{g,n+1}(t)|P_{-\ell}, g, n+1\rangle \right) \right), \end{aligned} \tag{23}$$

with $C_\ell^{e,n}(t)$, $C_\ell^{g,n+1}(t)$, $C_{-\ell}^{e,n}(t)$, and $C_{-\ell}^{g,n+1}(t)$ representing the time-dependent probability amplitudes for the atom. The probability amplitudes to find an atom in the state $|P_\ell\rangle$ satisfy the following equations, which may be derived in the Bragg regime from the Schrödinger equation,

$$i\frac{\partial C_\ell^{e,n}(t)}{\partial t} = (\Delta_0 \ell + \omega_{\text{rec}} \ell^2) C_\ell^{e,n}(t) + \frac{1}{2} g\sqrt{n+1} \left(C_{\ell+1}^{g,n+1}(t) + C_{\ell-1}^{g,n+1}(t) \right), \tag{24}$$

$$i\frac{\partial C_\ell^{g,n+1}(t)}{\partial t} = (\Delta_0 \ell + \omega_{\text{rec}} \ell^2) C_\ell^{g,n+1}(t) + \frac{1}{2} g\sqrt{n+1} \left(C_{\ell+1}^{e,n} + C_{\ell-1}^{e,n}(t) \right), \tag{25}$$

where the initial conditions read $C_{\ell_0}^{e,n}(0) = C_{-\ell_0}^{e,n}(0) = 1$ and $C_\ell^{g,n+1}(0) = C_{-\ell}^{g,n+1}(0) = 0$.

The analytical solution of differential equations (24) and (25) can be obtained in the Raman–Nath regime if the interaction time is very short. This regime of atomic diffraction is a characteristic of the situation where the recoil energy is smaller than the interaction energy [25], i.e.,

$$\omega_{\text{rec}} \ll g\sqrt{n+1}. \tag{26}$$

The analytical solutions of Eqs. (24) and (25) [26] are given by

$$C_{2\ell}^{e,n}(t) = \exp(-i(\Delta_0 t + \pi)\ell) J_{2\ell}(\xi(t)), \tag{27}$$

$$C_{2\ell+1}^{g,n+1}(t) = \exp(-i(\Delta_0 t + \pi)(\ell + 1/2)) J_{2\ell+1}(\xi(t)), \tag{28}$$

where J_ℓ is the ℓth-order Bessel function, $\xi(t) = [2g\sqrt{n+1}/\Delta_0] \sin(\Delta_0 t/2)$, and all the other probability amplitudes are zero.

In the case $P_{\ell_0} \neq 0$ and $\Delta_0 \neq 0$, the probability amplitudes $C_\ell^{e,n}(t)$ and $C_\ell^{g,n+1}(t)$ are periodic functions with the period

$$T = 2\pi/\Delta_0 = \lambda/v_0, \tag{29}$$

where $\lambda = 2\pi/k$ is the wavelength of the field and $v_0 = P_{\ell_0}/M$ is the velocity of the atomic motion along the cavity.

The same results are obtained for the atomic momentum states $|P_{-\ell}\rangle$.

The final atom–field state is then given by

$$\begin{aligned} |\psi(t)\rangle_{\text{final}} = & \frac{1}{\sqrt{2}} \sum_{\ell=-\infty}^{\infty} \left[\exp\left\{ -i \frac{P_{\ell_0}^2}{2M\hbar} t \right\} \left(C_{2\ell}^{e,n}(t)|P_{2\ell}, e, n\rangle + C_{2\ell+1}^{g,n+1}(t)|P_{2\ell+1}, g, n+1\rangle \right) \right. \\ & \left. + \exp\left\{ -i \frac{P_{-\ell_0}^2}{2M\hbar} t \right\} \left(C_{-2\ell}^{e,n}(t)|P_{-2\ell}, e, n\rangle + C_{-(2\ell+1)}^{g,n+1}(t)|P_{-(2\ell+1)}, g, n+1\rangle \right) \right]. \end{aligned} \tag{30}$$

This coherent superposition state of momentum gives the interference pattern at the screen. One can easily recover the initial state from Eq. (30). In fact, for $t = 0$, the initial momenta correspond to $\ell = 0$ and $\ell = -\ell_0$, $\xi(t = 0) = 0$, and $J_n(0) = \delta_{n,0}$, so that

$$|\psi(0)\rangle = \frac{1}{\sqrt{2}}(|P_{\ell_0}\rangle + |P_{-\ell_0}\rangle) \otimes |e, n\rangle. \tag{31}$$

The wave function of the atom with momentum P_ℓ, coming from the initial state of undiffracted beam, after interaction time t is given by

$$\begin{aligned}\psi_1(p_\ell, t) &= \frac{1}{\sqrt{2}} \exp\left\{-i\frac{P_0^2}{2M\hbar}t\right\} C_\ell^{e,n}(t)|e, n\rangle \quad \text{for} \quad \text{even} \quad \ell,\\ \psi_1(p_\ell, t) &= \frac{1}{\sqrt{2}} \exp\left\{-i\frac{P_0^2}{2M\hbar}t\right\} C_\ell^{g,n+1}(t)|g, n+1\rangle \quad \text{for} \quad \text{odd} \quad \ell.\end{aligned}$$

The wave function coming from the initial state of diffracted beam with momentum $P_{-\ell}$ after interaction time t is given by

$$\begin{aligned}\psi_2(p_\ell, t) &= \frac{1}{\sqrt{2}} \exp\left\{-i\frac{P_{-\ell_0}^2}{2M\hbar}t\right\} C_{-\ell}^{e,n}(t)|e, n\rangle \quad \text{for} \quad \text{even} \quad \ell,\\ \psi_2(p_\ell, t) &= \frac{1}{\sqrt{2}} \exp\left\{-i\frac{P_{-\ell_0}^2}{2M\hbar}t\right\} C_{-\ell}^{g,n+1}(t)|g, n+1\rangle \quad \text{for} \quad \text{odd} \quad \ell.\end{aligned}$$

The interference pattern is calculated as $\mathcal{P}(p_\ell, t) = |\psi_1(p_\ell, t) + \psi_2(p_\ell, t)|^2$, where $\psi_1(p_\ell, t)$ and $\psi_2(p_\ell, t)$ are the wave functions of the atomic center-of-mass motion in paths 1 and 2, respectively. Thus, the quantum interference is the result of an uncertainty in the path. The probability to find the atom with the momentum $\ell\hbar k$ is

$$\mathcal{P}(p_\ell, t) = \frac{1}{2}|J_\ell(\xi)|^2 \left(1 + \cos[2(\Delta_0 t + \pi)\ell]\right). \tag{32}$$

The interference behavior is represented by the term $\cos(2\Delta_0 t\ell)$, and the Bessel function $J_\ell(\xi)$ is explained as the envelop function of the fringes, which is varying slowly with time and atomic momentum (see Fig. 3) with $\Delta_0 = 1.63 \cdot 10^8$ Hz and $2g\sqrt{n+1}/\Delta_0 = 20$ [27]. The probability of atomic momentum of Eq. (32) shows that the atomic momentum is characterized by a symmetric distribution with respect to the axes $\ell\hbar k$ and $-\ell\hbar k$ (see Fig. 4). The distribution of the atomic momentum in the positive axis can exhibit the interference by the fringes with different intensities detected at the screen.

From Eq. (32), one can see that the evolution of the probability distribution varies periodically with the interaction time t, due to the parameter ξ. If the interaction time is an integer multiple of the period, $C_0^{e,n}(t) = 1$, while all the other probability amplitudes are zero. So, the atom completes full cycles and leaves the cavity in an excited state without contributing to the cavity field. Also, the probability decreases towards the minimum intensity in $\Delta_0 t/2 = k\pi/2$, with k an integer.

In Fig. 5, we show the atomic momentum distribution $\mathcal{P}(p_\ell, t)$ as a function of ℓ at different times, such as $t = (\pi/4)(1/\Delta_0)$, $(\pi/2)(1/\Delta_0)$, π/Δ_0, and $(3\pi/2)(1/\Delta_0)$. We observe that with increase in the time of interaction inside the cavity, the fringes of interference in the screen also increase (see Fig. 5b and d). We observe also that the range of the intensity peaks becomes wider with time.

Now, we are in a position to describe the loss of quantum interference in the presence of an environment that is associated with a random phase. So, decoherence affects the undiffracted/diffracted beams of the atom in the path to the second cavity (see Fig. 2), which is the object of the next section.

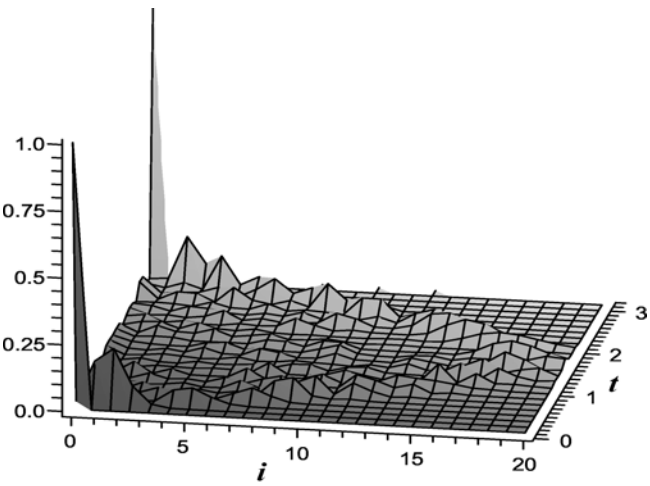

Fig. 3. Output momentum distribution of the atom scattered by the light standing wave of the cavity with different values of the probability to find the atom with the momentum $\ell\hbar k$ at time t.

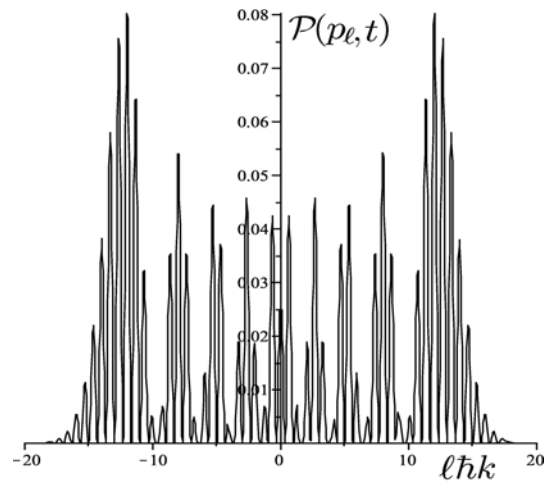

Fig. 4. Variation of the atomic momentum state for the Fock state as a function of ℓ from $-20\,\hbar k$ to $20\,\hbar k$ with time $t = 3\pi/2\Delta_0$ and $n = 50$.

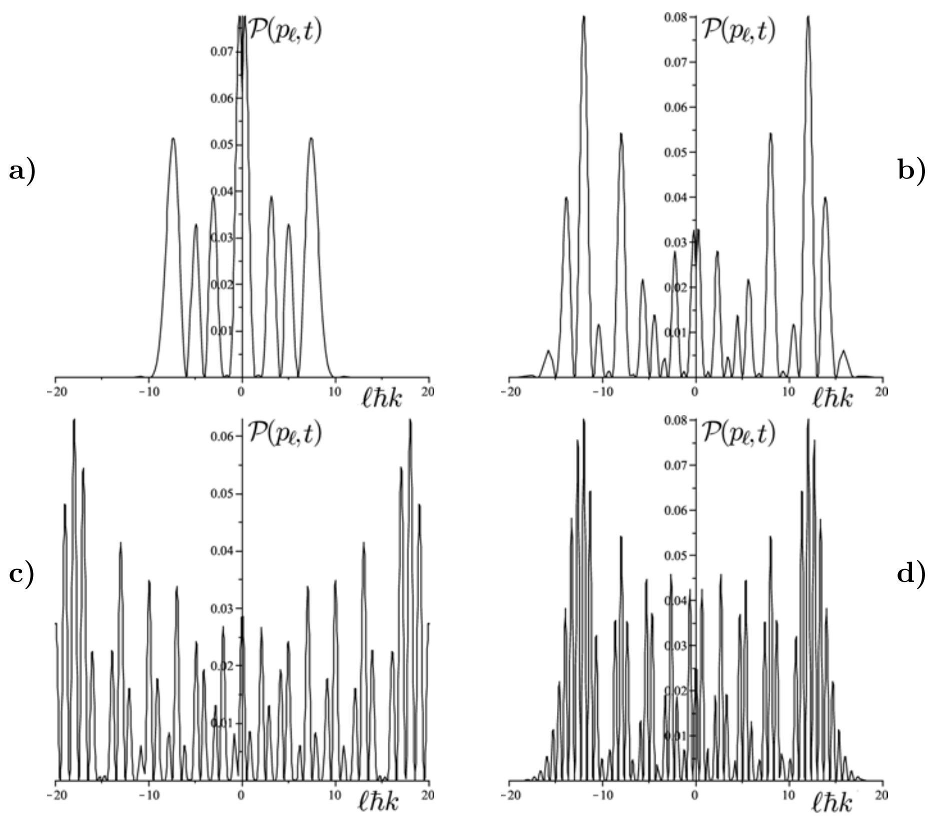

Fig. 5. Variation of atomic momentum state as a function of ℓ from $-20\,\hbar k$ to $20\,\hbar k$ with different times $t = (\pi/4)(1/\Delta_0)$ (a), $(\pi/2)(1/\Delta_0)$ (b), π/Δ_0 (c), and $(3\pi/2)(1/\Delta_0)$ (d).

3. Random Phase

We consider the case where the atomic beam coming out of the first cavity is incoherent, and two independent random phases are attached to the wave functions $\psi_1(p_\ell,t)$ and $\psi_2(p_\ell,t)$, respectively. The same result will hold if we study a random phase only at one wave function. So, a random phase is placed before the second cavity in the path of the atomic momentum state $|P_{\ell_0}\rangle$, and the state becomes $e^{i\phi}|P_{\ell_0}\rangle$ with the phase ϕ. After passing through the first cavity, the state reads

$$|\psi(t)\rangle = |P_{-\ell_0}\rangle + e^{i\phi}|P_{\ell_0}\rangle. \tag{33}$$

Assuming the previous scheme (Fig. 2), the atom–field state after the second cavity is

$$|\psi(t)\rangle = \frac{1}{\sqrt{2}}\sum_{\ell=-\infty}^{\infty}\left[\exp\left\{-i\frac{P_{\ell_0}^2}{2M\hbar}t\right\}e^{i\phi}\left(C_{2\ell}^{e,n}(t)|P_{2\ell},e,n\rangle + C_{2\ell+1}^{g,n+1}(t)|P_{2\ell+1},g,n+1\rangle\right)\right.$$
$$\left. +\exp\left\{-i\frac{P_{-\ell_0}^2}{2M\hbar}t\right\}\left(C_{-2\ell}^{e,n}(t)|P_{-2\ell},e,n\rangle + C_{-(2\ell+1)}^{g,n+1}(t)|P_{-(2\ell+1)},g,n+1\rangle\right)\right]. \tag{34}$$

After passing the cavity, the atomic beam propagates onto the screen, where the probability to find the atomic momentum $\ell\hbar k$ is given by

$$\mathcal{P}_\phi(p_\ell,t) = \frac{1}{2}|J_\ell(\xi)|^2(1+\cos(2\Delta_0 t\ell+\phi)). \tag{35}$$

Obviously, the interference and the phase behavior are represented by the term $\cos(2\Delta_0 t\ell+\phi)$, and the disappearance of this term means suppression of the atomic interference. So, the decoherence decreases the efficiency of quantum information for the atom from the quantum domain to the classical domain. The phase ϕ takes all values randomly, from 0 to 2π, and serves to destroy the interference completely,

$$\frac{1}{2\pi}\int_0^{2\pi}\mathcal{P}_\phi(p_\ell,t)\,d\phi = 1. \tag{36}$$

In fact, ϕ is a statistical variable, which is described by a distribution function $P(\phi)$. Hence, there are many assumptions on the distributions describing a random phase, e.g., the Gaussian distribution.

The probability distribution after detection at the screen is given by

$$\mathcal{P}(p_\ell,t) = \frac{1}{\sqrt{4\pi\sigma}}\int_0^{2\pi}e^{-\phi^2/4\sigma}\mathcal{P}_\phi(p_\ell,t)\,d\phi = \frac{1}{2}|J_\ell(\xi)|^2(1+\cos(2\Delta_0 t\ell)e^{-\sigma}), \tag{37}$$

where σ is a noise factor. The increase in this factor can suppress the interference phenomenon completely (see Fig. 6). So, one can destroy or recover the atom interference by increasing or decreasing the noise factor σ. It is the same effect we observe as we obtain the which-path information. Hence, we may conclude that the process of extracting which-path information leads to introducing a random phase. Also one can say that the control of the phase angle ϕ represents a switch that allows one to turn the interference fringes on and off.

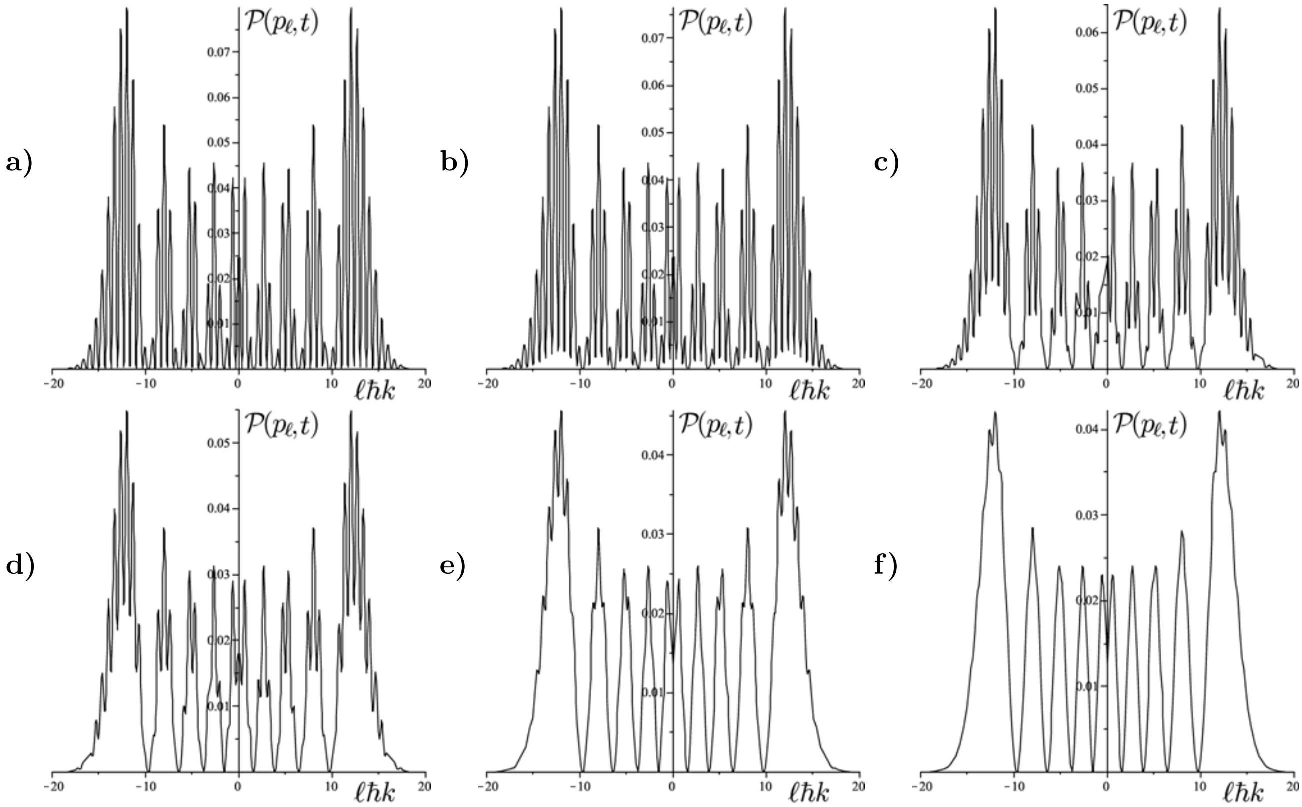

Fig. 6. Destruction of the atom interference by increasing the noise factor $\sigma = 0.01$ (a), 0.1 (b), 0.5 (c), 1 (d), 2 (e), and 3 (f), which decreases the contrast of fringes.

4. Conclusions

We have presented a model using the two-level atom with the field inside the cavities. The model was studied in two regimes — the Bragg regime and the Raman–Nath regime. The model elaborated allows one to obtain the atom interference using the atomic external degrees of freedom, such as an interferometer. We studied the loss of quantum interference of two paths under the influence of an environment and a random phase. We showed that, with increase in the randomness in an added phase, one switches from the quantum domain to the classical domain. It was the same effect we observed as we obtain the which-path information. Hence, we may conclude that the process of extracting which-path information leads to introducing a random phase, and this may help to solve the puzzle of which-path information.

Acknowledgments

A.E.A. acknowledges the hospitality of the Abdus Salam International Center for Theoretical Physics (Trieste, Italy) and thanks Prof. A. Benyoussef for previous discussions on the subject. F.S. acknowledges partial support of Pró-Reitoria de Pesquisa-UNESP, Sao Paulo and HEC NRP 20-1374, Pakistan.

References

1. N. Bohr, *Quantum Theory and Measurement*, J. A. Wheeler and W. H. Zurker (eds.), Princeton University Press, Princeton, NJ (1983), p. 9.
2. R. P. Feynman, R. Leughton, and M. Sands, *The Feynman Lectures on Physics*, Addison-Wesly, Reading, MA (1965).
3. M. O. Scully and K. Drühl, *Phys. Rev. A*, **25**, 2208 (1982).
4. A. Stern, Y. Aharonov, and Y. Imry, *Phys. Rev. A*, **41**, 3436 (1990).
5. M. O. Scully, B. G. Englert, and H. Walther, *Nature*, **351**, 111 (1991).
6. S. Dürr, T. Nonn, and G. Rempe, *Nature*, **395**, 33 (1998).
7. P. Bertet, S. Osnaghi, A. Rauschenbeutel, et al., *Nature*, **411**, 166 (2001).
8. S.P. Walborn, M. O. Terra Cunha, S. Pádua and C. H. Monken, *Phys. Rev. A*, **65**, 033818 (2002).
9. L. Neves, G. Lima, J. Aguirre, et al., *New J. Phys.* **11**, 073035 (2009).
10. M. Davidovic, A. S. Sanz, M. Bozic, and D. Arsenovic, "Loss, revival, and regain of atomic interference: An explanation grounded on the momentum transfer during photon–atom scattering events," Los Alamos ArXiv:1006.0450v1.
11. C. Ferrari and B. Braunecker, *Am. J. Phys.*, **78**, 792 (2010).
12. U. Schilling and J. von Zanthier, "Phase-dependent which-way information," Los Alamos ArXiv:1102.5709v1.
13. Y. Aharonov and M. S. Zubairy, *Science*, **307**, 875 (2005).
14. N. Metwally, *Int. J. Theor. Phys.*, **49**, 1571 (2010).
15. N. Metwally, "Dynamics of information in the presence of deformation," Los Alamos ArXiv:1006.4805.
16. T. Abbas, R. Islam, A. H. Khosa, and F. Saif, *J. Russ. Laser Res.*, **30**, 267 (2009).
17. F. Saif, R. Islam, and A. H. Khosa, *J. Phys. B: At. Mol. Opt. Phys.*, **43**, 015501 (2010).
18. A. El Allati, Y. Hassouni, and F. Saif, "Deterministic secure communication via atomic momentum state," DOI10.1016/j.ijleo.2010.12.013.
19. A. F. Bernhardt and B. W. Shore, *Phys. Rev. A*, **23**, 1290 (1981).
20. M. Marte and S. Stenholm, *Appl. Phys. B*, **54**, 443 (1992).
21. A. Khalique and F. Saif, *Phys. Lett. A*, **314**, 37 (2003).
22. R. J. Cook and A. F. Bernhardt, *Phys. Rev. A*, **18**, 2533 (1978).
23. C. M. Savage, S. L. Braunstein, and D. F. Walls, *Opt. Lett.*, **15**, 628 (1990).
24. P. Meystre, E. Schumacher, and S. Stenholm, *Opt. Commun.*, **73**, 443 (1989).
25. E. Mayr, D. Krähmer,A. M. Herkommer, et al., *Acta Phys. Pol. A*, **85**, 483 (1994).
26. M. O. Scully and W. E. Lamb, *Phys. Rev.*, **159**, 208 (1967).
27. J. S. Peng and G. X. Li, *Intoduction to Modern Quantum Optics*, World Scientific Publishing Company, Cambridge University Press (1998), p. 471.